

B-Methylated Amine-Boranes: Substituent Redistribution, Catalytic Dehydrogenation, and Facile Metal-Free Hydrogen Transfer Reactions

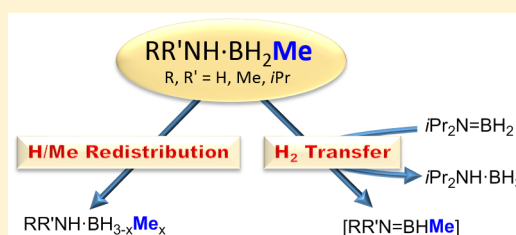
Naomi E. Stubbs, André Schäfer, Alasdair P. M. Robertson, Erin M. Leita, Titil Jurca, Hazel A. Sparkes, Christopher H. Woodall, Mairi F. Haddow, and Ian Manners*

School of Chemistry, University of Bristol, Cantock's Close, Bristol, BS8 1TS, U.K.

S Supporting Information

ABSTRACT: Although the dehydrogenation chemistry of amine-boranes substituted at nitrogen has attracted considerable attention, much less is known about the reactivity of their B-substituted analogues. When the B-methylated amine-borane adducts, $RR'NH \cdot BH_2Me$ (**1a**: $R = R' = H$; **1b**: $R = Me, R' = H$; **1c**: $R = R' = Me$; **1d**: $R = R' = iPr$), were heated to 70 °C in solution (THF or toluene), redistribution reactions were observed involving the apparent scrambling of the methyl and hydrogen substituents on boron to afford a mixture of the species $RR'NH \cdot BH_{3-x}Me_x$ ($x = 0-3$).

These reactions were postulated to arise via amine-borane dissociation followed by the reversible formation of diborane intermediates and adduct reformation. Dehydrocoupling of **1a–1d** with Rh(I), Ir(III), and Ni(0) precatalysts in THF at 20 °C resulted in an array of products, including aminoborane $RR'N=BHMe$, cyclic diborazane $[RR'N-BHMe]_2$, and borazine $[RN-BMe]_3$ based on analysis by in situ ^{11}B NMR spectroscopy, with peak assignments further supported by density functional theory (DFT) calculations. Significantly, very rapid, metal-free hydrogen transfer between **1a** and the monomeric aminoborane, $iPr_2N=BH_2$, to yield $iPr_2NH \cdot BH_3$ (together with dehydrogenation products derived from **1a**) was complete within only 10 min at 20 °C in THF, substantially faster than for the N-substituted analogue $MeNH_2 \cdot BH_3$. DFT calculations revealed that the hydrogen transfer proceeded via a concerted mechanism through a cyclic six-membered transition state analogous to that previously reported for the reaction of the N-dimethyl species $Me_2NH \cdot BH_3$ and $iPr_2N=BH_2$. However, as a result of the presence of an electron donating methyl substituent on boron rather than on nitrogen, the process was more thermodynamically favorable and the activation energy barrier was reduced.



1. INTRODUCTION

Amine-boranes ($RR'R''N \cdot BH_3$, $R, R', R'' = H$, alkyl or aryl) are isoelectronic with alkanes and have been the recent focus of intense attention as a result of their potential applications in hydrogen storage and transfer, as well as precursors to new inorganic materials.¹ For example, polyaminoboranes, $[RNH-BH_2]_n$, which are structurally analogous and isoelectronic to polyolefins, represent an interesting class of polymers accessed from amine-boranes that may possess useful piezoelectric or preceramic properties.² Dehydrocoupling of amine-boranes, where the release of hydrogen is accompanied by the formation of new B–N bonds, can be performed thermally,^{1c} using stoichiometric amounts of a hydrogen acceptor,^{1i–1j} or much more efficiently with a variety of Rh,⁴ Ir,^{2d,5} Ni,⁶ Ti,⁷ Fe,^{6c,8} Re,⁹ or Ru¹⁰ precatalysts as well as with other transition metal¹¹ and main-group species.¹² Under these conditions, ammonia-borane, $NH_3 \cdot BH_3$, as well as primary amine-boranes, $RNH_2 \cdot BH_3$, and secondary amine-boranes, $RR'NH \cdot BH_3$ ($R, R' = \text{alkyl, aryl}$) readily eliminate one equivalent of hydrogen to yield aminoboranes, $RR'N=BH_2$, which can either be stable as a monomer or undergo oligomerization to yield linear $RR'NH-[BH_2-RR']_x-BH_3$ or cyclic $[RR'N-BH_2]_x$ borazines ($x = 2$ or 3) (Scheme 1).¹³ Alternatively, high molecular weight

polyaminoboranes, $[RNH-BH_2]_n$, can be formed if the precursor is ammonia-borane ($R = H$) or a sterically unhindered primary amine-borane ($R = Me, Et, nBu$) and the catalyst is selective for dehydropolymerization.^{2d,4e,5c,6a,14}

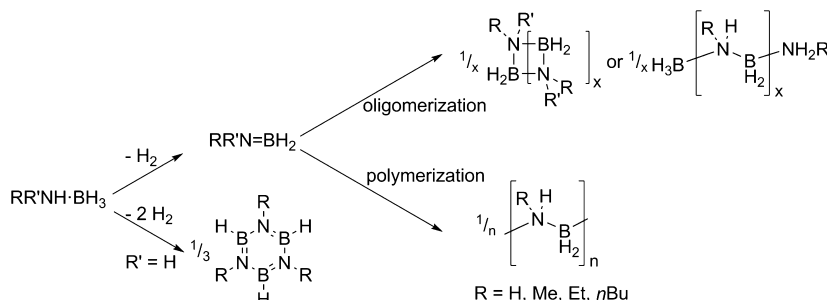
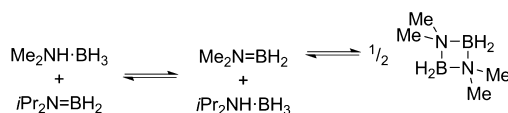
Under most circumstances, elimination of two equivalents of hydrogen occurs with ammonia-borane and primary amine-boranes to yield borazines, $[RN-BH]_3$ (Scheme 1).¹⁵

In recent years amine-boranes have been shown to function as hydrogen donors providing one or more equivalents of hydrogen to acceptors such as imines,^{1k} olefins,^{1l,2c,d} aminoboranes,^{1j} a C_4 cumulene,¹⁶ and azobenzene.¹⁷ We have recently reported detailed kinetic and thermodynamic studies of the hydrogen transfer reaction of $Me_2NH \cdot BH_3$ and $iPr_2N=BH_2$ to yield $Me_2N=BH_2$ and $iPr_2NH \cdot BH_3$, where the former aminoborane subsequently dimerizes to form $[Me_2N-BH_2]_2$ (Scheme 2). Experimental data and density functional theory (DFT) calculations determined that the hydrogen transfer step was slightly endergonic ($\Delta G^\circ_{\text{exp}} = +10 \pm 7 \text{ kJ mol}^{-1}$, $\Delta G^\circ_{\text{calc}} = +9.1 \text{ kJ mol}^{-1}$) with the dimerization of $Me_2N=BH_2$ providing the driving force for the overall reaction ($\Delta G^\circ_{\text{exp}} = -28 \pm 14 \text{ kJ}$

Received: August 24, 2015

Published: November 4, 2015

Scheme 1. Dehydrocoupling of Amine-Boranes

Scheme 2. Hydrogen Transfer between $\text{Me}_2\text{NH}\cdot\text{BH}_3$ and $i\text{Pr}_2\text{N}=\text{BH}_2$ 

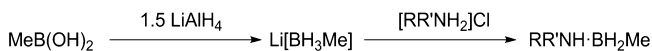
mol^{-1} , $\Delta G^\circ_{\text{calc}} = -20.0 \text{ kJ mol}^{-1}$).^{1j} The mechanistic pathway for the hydrogen transfer was investigated and found to involve a concerted process with a cyclic six-membered transition state and an activation energy of $+91 \pm 5 \text{ kJ mol}^{-1}$ ($\Delta G^\ddagger_{\text{exp}}$) or $+86.9 \text{ kJ mol}^{-1}$ ($\Delta G^\ddagger_{\text{calc}}$).

Although a wide range of N-substituted amine-boranes are known and have been investigated extensively,^{4a} to date, far fewer examples of B-substituted amine-boranes have been studied. The geometries and dissociation energies of NH_3 , $\text{BH}_x\text{Me}_{3-x}$ and $\text{Me}_x\text{NH}_{3-x}\cdot\text{BH}_3$ ($x = 0-3$) were theoretically predicted by Boutalib and co-workers, who suggested that the stability of the amine-borane increased upon inclusion of a methyl group at nitrogen with a corresponding decrease when boron possessed methyl substituents.¹⁸ Dixon and co-workers investigated the dehydrogenation energies of the same set of amine-boranes via DFT calculations and reported that having a methyl substituent at boron led to an exothermic dehydrogenation reaction, whereas at nitrogen the process was close to thermoneutral.¹⁹ In addition, our group has previously reported that the B-pentafluorophenyl substituted amine-borane, $i\text{Pr}_2\text{NH}\cdot\text{BH}(\text{C}_6\text{F}_5)_2$, undergoes thermal dehydrogenation at 100°C to yield the aminoborane $i\text{Pr}_2\text{N}=\text{B}(\text{C}_6\text{F}_5)_2$.²⁰ We have also synthesized a series of B-thioaryl substituted amine-boranes, including $i\text{Pr}_2\text{NH}\cdot\text{BH}_2\text{SR}$ ($\text{R} = \text{Ph}, \text{C}_6\text{F}_5$), which underwent both thermal and catalytic dehydrogenation to yield B-thioaryl substituted aminoborane, $i\text{Pr}_2\text{N}=\text{BHSR}$.²¹ Synthesis of two B-methylated amine-boranes, $\text{Me}_3\text{N}\cdot\text{BH}_2\text{Me}$ and $\text{Me}_2\text{NH}\cdot\text{BH}_2\text{Me}$, has been previously reported by Paul and Roberts,²² and Beachley and Washburn,²³ although no further studies of their reactivity were described.

Herein, we report the synthesis of a series of B-methylated amine-boranes (**1a**, $\text{NH}_3\cdot\text{BH}_2\text{Me}$; **1b**, $\text{MeNH}_2\cdot\text{BH}_2\text{Me}$; **1c**, $\text{Me}_2\text{NH}\cdot\text{BH}_2\text{Me}$; **1d**, $i\text{Pr}_2\text{NH}\cdot\text{BH}_2\text{Me}$) and describe studies of their reactivity at elevated temperatures as well as toward a range of well-established dehydrocoupling catalysts and the hydrogen acceptor, $i\text{Pr}_2\text{N}=\text{BH}_2$. While our work was in progress, Liu and co-workers independently reported the synthesis of **1a** and **1b**, and determined that the catalytic dehydrocoupling of these species in the presence of CoCl_2 at 80°C yielded borazine, $[\text{RN}-\text{BMe}]_3$ ($\text{R} = \text{H}$ or Me) as the sole product after 36 h.^{11d}

2. RESULTS

2.1. Synthesis and Characterization of 1a–1d. The synthesis of a series of B-methylated amine-boranes (**1a–1d**) was carried out via salt metathesis with $\text{Li}[\text{BH}_3\text{Me}]$ and $[\text{RR}'\text{NH}_2]\text{Cl}$ ($\text{R}, \text{R}' = \text{H}, \text{Me}$, or $i\text{Pr}$, Scheme 3).^{11d} The former species was prepared by the reaction of $\text{MeB}(\text{OH})_2$ with 1.5 equivalents of LiAlH_4 .²⁴

Scheme 3. Synthesis of B-Methylated Amine-Boranes **1a–1d** (**1a**: $\text{R}, \text{R}' = \text{H}$; **1b**: $\text{R} = \text{H}, \text{R}' = \text{Me}$; **1c**: $\text{R}, \text{R}' = \text{Me}$; **1d**: $\text{R}, \text{R}' = i\text{Pr}$)

The B-methylated amine-boranes were isolated as either colorless solids (**1a**, **1b**, **1d**) or as a liquid (**1c**), and selected characterization data is given in Table 1.²⁵ As expected, one signal was observed in the ^{11}B NMR spectra in the range -8.5 to -15.1 ppm as a triplet ($J_{\text{BH}} = 94-96 \text{ Hz}$), for **1a–1d** in CDCl_3 (Figures S1, S3, S6, and S9). The observed chemical shift and coupling pattern was indicative of a four-coordinate boron center with two hydrogen substituents. Comparison of the ^{11}B NMR chemical shifts of **1a–1d** to the analogous amine-boranes—ammonia-borane, $\text{NH}_3\cdot\text{BH}_3$; N-methyl amine-borane, $\text{MeNH}_2\cdot\text{BH}_3$; N-dimethyl amine-borane, $\text{Me}_2\text{NH}\cdot\text{BH}_3$; and N-diisopropyl amine-borane, $i\text{Pr}_2\text{NH}\cdot\text{BH}_3$ —indicated that a downfield shift was observed upon the replacement of a hydrogen for a methyl group at boron (Table 1).^{4a} The observed ^1H (Figures S2, S4, S7, and S10) and ^{13}C (Figures S5, S8, and S11) NMR spectra were unremarkable, but consistent with the assigned structures.

Recrystallization of **1a** from a solution of Et_2O /hexanes at -40°C yielded small, colorless crystals suitable for study by single crystal X-ray diffraction, which corroborated the connectivity suggested by the other spectroscopic data (Figure 1a).²⁵ In an analogous fashion, crystals of **1b** and **1d** were grown that were also suitable for X-ray diffraction (Figures 1b and 2).²⁵

The B–N bond length for **1a** was determined to be $1.614(3) \text{ \AA}$, which was similar to that of **1b** ($1.605(2) \text{ \AA}$) within experimental error (Table 2). On the other hand, the inclusion of two sterically bulky isopropyl groups at nitrogen (in **1d**) significantly lengthened the B–N bond to $1.6333(6) \text{ \AA}$. Although the increased electron donating ability of the isopropyl groups would be expected to strengthen the dative bond, the steric effect of the bulky alkyl groups dominates, thereby weakening the B–N bond. The B–N bond length for $\text{NH}_3\cdot\text{BH}_3$ was determined to be $1.58(2)$ ²⁷ by neutron diffraction, which was considered similar to that observed for

Table 1. Yields and ^{11}B and ^1H NMR Spectroscopic Data of Selected Amine-Boranes in CDCl_3 ^{4a,26}

amine-borane	yield/%	δ_{B}	J_{BH}	$\delta_{\text{H}}(\text{B}-\text{CH}_3)$	$\delta_{\text{H}}(\text{N}-\text{CH})$	ref
$\text{NH}_3\cdot\text{BH}_3$	86	−21.6	95	—	—	4a
1a	41	−15.1	95	−0.11	—	this work
$\text{MeNH}_2\cdot\text{BH}_3$	89	−18.8	94	—	2.54	4a
1b	46	−12.3	93	−0.18	2.52	this work
$\text{Me}_2\text{NH}\cdot\text{BH}_3$	71	−15.1	96	—	2.59	26
1c	18	−8.5	94	−0.19	2.55	this work
$i\text{Pr}_2\text{NH}\cdot\text{BH}_3$	90	−21.1	97	—	3.23	4a
1d	31	−14.6	96	−0.18	3.34	this work

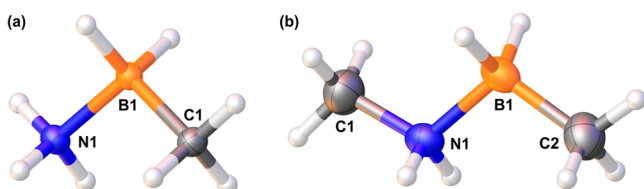
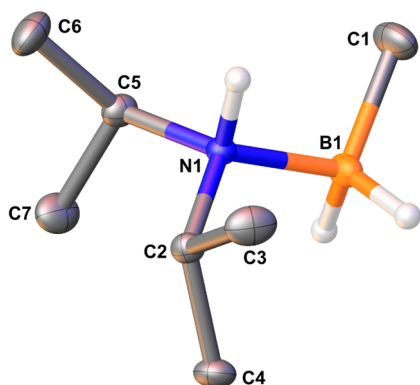
Figure 1. Molecular structure of compounds (a) **1a** and (b) **1b** with all non-H atom thermal ellipsoids drawn at the 50% probability level.Figure 2. Molecular structure of compound **1d** with all non-H atom thermal ellipsoids drawn at the 50% probability level. All hydrogen atoms bonded to carbon were omitted for clarity.

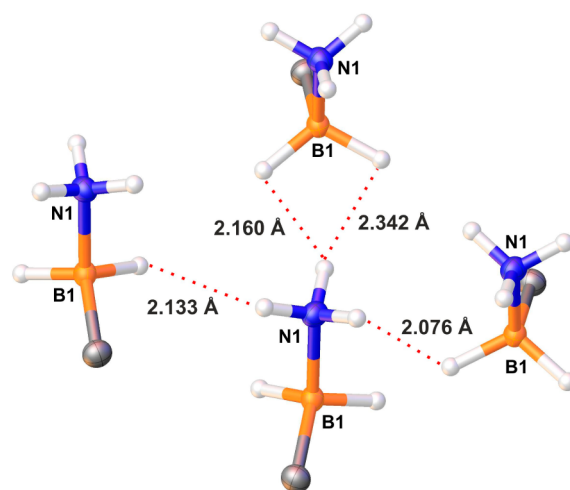
Table 2. B–N Bond Lengths of Selected Amine-Boranes by X-ray Diffraction

amine-borane	B–N bond length/Å	ref
$\text{NH}_3\cdot\text{BH}_3$	1.58(2) ^a	27
1a	1.614(3)	this work
$\text{MeNH}_2\cdot\text{BH}_3$	1.5936(13)	28
1b	1.605(2)	this work
$\text{Me}_2\text{NH}\cdot\text{BH}_3$	1.5965(13)	28
1d	1.6333(6)	this work

^aDetermined by neutron diffraction.

the amine-boranes **1a**, **1b**, and **1d**. However, a significantly longer B–N bond length was found compared to the analogous amine-boranes without a methyl group at boron (1.5936(13) and 1.5965(13) Å for $\text{MeNH}_2\cdot\text{BH}_3$ and $\text{Me}_2\text{NH}\cdot\text{BH}_3$, respectively),²⁸ as determined by X-ray diffraction. This was likely a consequence of an increase in electron density at boron induced by the electron donating methyl group, which reduced the strength of the B–N dative bond. Both the boron and nitrogen atoms of **1b** were found to exhibit distorted tetrahedral geometries, consistent with approximate sp^3 hybridization, and the C1–N1–B1–C2 chain was found to adopt a gauche conformation with a dihedral angle of 178.27°.

Longer-distance, noncovalent intermolecular interactions were observed for **1a** between adjacent amine-boranes, with lengths in the range 2.08–2.34 Å between the hydridic and protic hydrogen atoms on boron and nitrogen, respectively (Figure 3 and Table 3). These distances were shorter than

Figure 3. Association of the molecules of **1a** via dihydrogen intermolecular interactions in the solid state with thermal ellipsoids at the 50% probability level. All hydrogen atoms bonded to carbon are omitted for clarity.Table 3. H–H Bond Distances ($D(\text{H}_{\text{N}}-\text{H}_{\text{B}})$) and Angles ($\angle\text{HHN}$ and $\angle\text{HHB}$) between Protic and Hydridic Hydrogens on B-Methylated Amine-Boranes **1a**, **1b**, and **1d**

amine-borane	$D(\text{H}_{\text{N}}-\text{H}_{\text{B}})/\text{Å}$	$\angle\text{HHN}/\text{deg}$	$\angle\text{HHB}/\text{deg}$
1a	2.076	161.9	147.4
	2.133	140.5	123.4
	2.160	143.6	102.4
	2.342	167.2	92.6
1b	2.253	137.5	94.9
	2.130	166.0	99.3
	2.119	151.9	131.0
1d	2.163	174.2	144.1

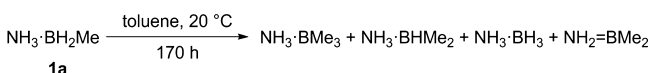
twice the van der Waals radius for two hydrogen atoms (2.4 Å). Dihydrogen intermolecular interactions were also detected for amine-boranes **1b** and **1d** (Figures S61 and S62 and Table 3). The H–H–N angles were determined to be relatively linear (137.6–174.2°), in contrast to the corresponding H–H–B angles indicating a bent geometry, with values in the range 92.7–147.4°. Together with the dihydrogen distances, these types of linear H–H–N bond and bent H–H–B bond geometry were similar to those observed for dihydrogen

intermolecular interactions in other crystallographically characterized amine-boranes.^{27–29}

2.2. Thermally Induced Redistribution and Dehydrogenation Reactions of 1a–1d. To determine the thermal stability of the B-methylated amine-boranes, a solution of **1a–1d** in either a coordinating (tetrahydrofuran, THF) or a weakly coordinating (toluene) solvent was monitored by ¹¹B NMR spectroscopy at ambient (20 °C) and elevated (70 °C) temperatures over various periods of time. The assignment of the product signals detected by ¹¹B NMR spectroscopy was further supported by literature chemical shift data ($\delta_{\text{B,lit}}$), where available, as well as DFT calculations of ¹¹B NMR chemical shifts ($\delta_{\text{B,calc}}$) and ¹J_{BH} coupling constants (Table S4).²⁵

2.2.1. Thermally Induced Redistribution and Dehydrogenation Reactions of 1a. The thermal stability of **1a** at ambient temperature was investigated by ¹¹B NMR spectroscopy. No reaction was observed for **1a** in a THF solution after 170 h at 20 °C (Figure S16). However, under analogous conditions in a toluene solution, significant amounts of products derived from the redistribution of the methyl and hydrogen substituents at boron were observed; in addition to unreacted **1a** (ca. 40%), the appearance of singlet, doublet, and quartet peaks at –6.1, –9.5, and –22.3 ppm, respectively, were detected by ¹¹B NMR spectroscopy at 20 °C after 170 h. The product peaks were postulated to correspond to B-trimethyl amine-borane, NH₃·BMe₃ [$\delta_{\text{B,exp}}$ –6.1 (s)] [$\delta_{\text{B,calc}}$ –7.0] (ca. 10%), B-dimethyl amine-borane, NH₃·BHMe₂ [$\delta_{\text{B,exp}}$ –9.5 (d, ¹J_{BH} = 107 Hz)] [$\delta_{\text{B,calc}}$ –9.8 (¹J_{BH} = 97 Hz)] (ca. 30%), and NH₃·BH₃ [$\delta_{\text{B,exp}}$ –22.3 (q, ¹J_{BH} = 91 Hz)] [$\delta_{\text{B,lit}}$ –21.6 (q, ¹J_{BH} = 95 Hz)]^{4a} (ca. 10%) (Scheme 4, Figure S17).

Scheme 4. Redistribution of Methyl and Hydrogen Substituents at Boron for 1a in Toluene at 20 °C

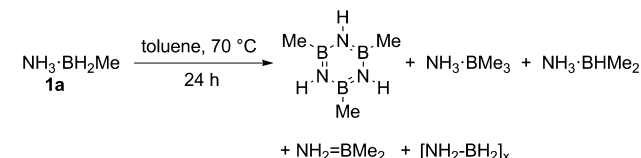


As well as the products arising from methyl and hydrogen redistribution at boron for **1a**, a broad ¹¹B NMR peak with no detectable proton coupling was observed at $\delta_{\text{B,exp}}$ 46.3 (s). This was assigned to B-dimethyl aminoborane, NH₂=BMe₂ [$\delta_{\text{B,calc}}$ 48.8] [$\delta_{\text{B,lit}}$ 47.1]³⁰ (ca. 10%), which was postulated to arise as a result of the instability of NH₃·BHMe₂ toward hydrogen loss, as predicted by DFT calculations.¹⁹

The redistribution reaction of **1a** in toluene was also studied at elevated temperature (70 °C). After 24 h, ¹¹B NMR spectroscopy showed that **1a** had been completely consumed with the formation of the dehydrocoupled product B-trimethyl borazine [NH–BMe]₃ [$\delta_{\text{B,exp}}$ 34.3 (s)] [$\delta_{\text{B,calc}}$ 34.5] [$\delta_{\text{B,lit}}$ 36.0]³¹ (ca. 10%). Other products observed were NH₂=BMe₂ (ca. 40%) and the redistribution product NH₃·BHMe₂ (ca. 30%). Minor amounts of NH₃·BMe₃ (ca. 10%), and [NH₂–BH₂]_x [$\delta_{\text{B,exp}}$ –13.9 (m)] [$\delta_{\text{B,lit}}$ –10.7 (in solid state)]^{5c} (ca. 10%) were also detected (Scheme 5, Figure S18). Similar redistribution products were observed when heating **1a** to 70 °C in THF after 24 h (Figure S19).

2.2.2. Thermally Induced Redistribution and Dehydrogenation Reactions of 1b–1d. In contrast to the redistribution of the methyl and hydrogen substituents at boron observed for **1a** in toluene at 20 °C, no corresponding reaction was detected for solutions of **1b–1d** in either coordinating (THF) or weakly coordinating (toluene) solvents after 170 h by ¹¹B NMR spectroscopy (Figures S20–S25). The stability of **1b–1d** at

Scheme 5. Thermolysis of 1a in Toluene at 70 °C

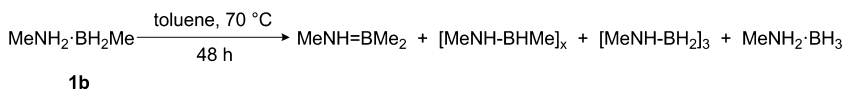
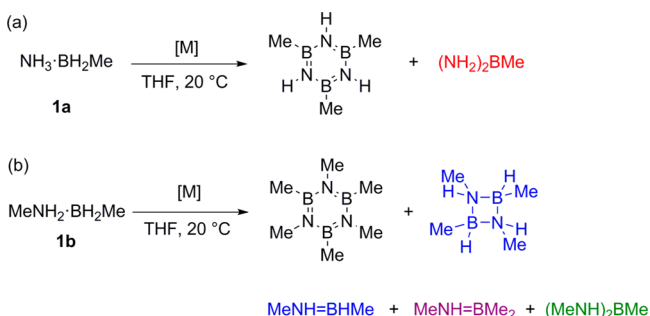


elevated temperatures was then investigated; a toluene solution of **1b–1d** was heated to 70 °C until quantitative consumption of the amine-borane was detected. As the steric bulk of the alkyl groups increased at nitrogen, the reaction time for complete consumption of the B-methylated amine-borane increased from 48 h (**1b**) to 170 h (**1c**) to 500 h (21 days) (**1d**), as monitored by ¹¹B NMR spectroscopy.

Similar to the case of **1a**, thermolysis of **1b** in toluene at 70 °C led to the formation of a complex mixture of redistribution and dehydrogenation products by ¹¹B NMR spectroscopy, although the process was slower (48 h). These products consisted of MeNH=BMe₂ [$\delta_{\text{B,exp}}$ 45.0 (s)] [$\delta_{\text{B,calc}}$ 47.4] [$\delta_{\text{B,lit}}$ 45.7]³⁰ (ca. 30%), tentatively assigned cyclic oligo(B-methyl aminoborane) [MeNH–BHMe]_x [$\delta_{\text{B,exp}}$ –3.2 (d, br)] (ca. 20%), N-trimethyl triborazane [MeNH–BH₂]₃ [$\delta_{\text{B,exp}}$ –7.0 (m)] [$\delta_{\text{B,lit}}$ –5.4 (t, ¹J_{BH} = 107 Hz)]³² (ca. 20%), and MeNH₂·BH₃ [$\delta_{\text{B,exp}}$ –18.4 (q, ¹J_{BH} = 96 Hz)] [$\delta_{\text{B,lit}}$ –18.8 (¹J_{BH} = 94 Hz)]^{4a} (ca. 30%) (Scheme 6, Figure S26). Analogous redistribution and dehydrogenation products were detected for the thermolysis reaction of **1c** (Figure S27), and for **1d**, only dehydrogenated derivatives *i*Pr₂N=BMe₂ [$\delta_{\text{B,exp}}$ 44.0 (s)] [$\delta_{\text{B,calc}}$ 47.2] (ca. 30%) and *i*Pr₂N=BHMe [$\delta_{\text{B,exp}}$ 39.2 (d, ¹J_{BH} = 119 Hz)] [$\delta_{\text{B,calc}}$ 41.4 (¹J_{BH} = 122 Hz)] (ca. 40%) were formed together with *i*Pr₂NH·BH₃ [$\delta_{\text{B,exp}}$ –21.4 (q, ¹J_{BH} = 99 Hz)] [$\delta_{\text{B,calc}}$ –21.1 (¹J_{BH} = 97 Hz)]^{4a} in toluene at 70 °C (Figure S28). Similar reactivity was also observed for the thermolysis of **1b–1d** in the more coordinating solvent, THF, at 70 °C over a period of 170–340 h (Figures S29–S31).

2.3. Catalytic Dehydrocoupling Reactions of B-Methylated Amine-Boranes 1a–1d. In an attempt to favor dehydrocoupling over redistribution reactions, the use of transition metal catalysts was explored. Specifically, the reactivity of the B-methylated amine-boranes **1a–1d** toward previously established dehydrocoupling catalysts [Rh(COD)(μ-Cl)]₂ (COD = 1,5-cyclooctadiene),^{4a} IrH₂(POCOP) (POCOP = κ³-1,3-(OPtBu₂)₂C₆H₃),^{2d,5a} and skeletal nickel^{6a} was investigated.

2.3.1. Catalytic Dehydrocoupling of 1a–1d with [Rh(COD)(μ-Cl)]₂. A THF solution of **1a** was treated with 2.5 mol % [Rh(COD)(μ-Cl)]₂ (5 mol % Rh) at 20 °C, and the reaction course was monitored by ¹¹B NMR spectroscopy. After 1 h, complete consumption of the starting material was observed with the quantitative formation of the dehydrocoupled product, B-trimethyl borazine [NH–BMe]₃ (Scheme 7a, Figure S32). The quantitative conversion was similarly reported by Liu and co-workers,^{11d} whereby **1a** in diglyme with 5 mol % CoCl₂ yielded borazine [NH–BMe]₃ with the exception that their reaction was heated at 80 °C and required 36 h to reach completion. Upon addition of [Rh(COD)(μ-Cl)]₂ to the THF solution of **1a–1d**, a change from a transparent yellow solution to a black suspension was observed. This was consistent with reduction of the Rh(I) precatalyst to rhodium colloids, the likely active catalyst based on previous studies on amine-borane dehydrocoupling with [Rh(COD)(μ-Cl)]₂.^{4a,33}

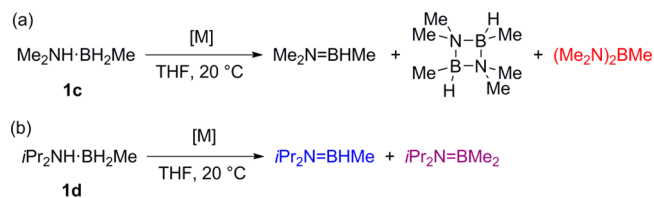
Scheme 6. Thermolysis of **1b** in Toluene at 70 °CScheme 7. Catalytic Dehydrocoupling of (a) **1a** and (b) **1b** in THF at 20 °C ([M] = 2.5 mol % [Rh(COD)(μ-Cl)]₂, 5 mol % IrH₂(POCOP), 10 mol % Skeletal Nickel)^{33a}

^aSpecies that appear with only specific substrates and precatalysts are labeled as follows: (red) with **1a** and IrH₂(POCOP) or skeletal nickel, (blue) with **1b** and IrH₂(POCOP) or skeletal nickel, (purple) with **1b** and skeletal nickel, and (green) with **1b** and [Rh(COD)(μ-Cl)]₂ or skeletal nickel.

In contrast to the rapid and quantitative dehydrocoupling reactivity observed for **1a**, the reaction of **1b** in THF at 20 °C with 2.5 mol % [Rh(COD)(μ-Cl)]₂ (5 mol % Rh) resulted in a slower conversion of the amine-borane (24 h for complete consumption). In this case, two products were formed: *B*-trimethyl-*N*-trimethyl borazane [MeN-BMe]₃ [$\delta_{\text{B,exp}}$ 35.7 (s)]³⁴ [$\delta_{\text{B,calc}}$ 36.4] (ca. 80%) and *B*-methyl-*N*-methylbis(amino)borane (MeNH)₂BMe [$\delta_{\text{B,exp}}$ 31.0 (s)] [$\delta_{\text{B,calc}}$ 30.2] [$\delta_{\text{B,lit}}$ 31.7]³⁰ (ca. 20%), as observed by ¹¹B NMR spectroscopy (Scheme 7b, Figure S33). In this case, the formation of the two products differs from the results described by Liu and co-workers for the Co-catalyzed dehydrogenation of **1b**, as under more forcing conditions (5 mol % CoCl₂, 80 °C, 36 h), borazine was observed as the sole product.^{11d}

The catalytic dehydrogenation of **1c** with 2.5 mol % [Rh(COD)(μ-Cl)]₂ (5 mol % Rh) in THF at 20 °C proceeded at a similar rate to that of **1b**, although the product mixture showed a further increase in complexity. Complete consumption of amine-borane was observed after 24 h with the formation of Me₂N=BHMe (ca. 30%), the corresponding dimer, cyclic *B*-dimethyl-*N*-tetramethyl diborazane, [Me₂N-BHMe]₂ [$\delta_{\text{B,exp}}$ 4.9 (d, ¹J_{BH} = 110 Hz) and 4.4 (d, ¹J_{BH} = 109 Hz)] [$\delta_{\text{B,calc}}$ 2.4 (¹J_{BH} = 110 Hz)] (ca. 40%), and *B*-methyl-*N*-dimethylbis(amino)borane, (Me₂N)₂BMe [$\delta_{\text{B,exp}}$ 30.3 (s)] [$\delta_{\text{B,calc}}$ 33.5] (ca. 20%) together with an unidentified product [$\delta_{\text{B,exp}}$ 3.8 (m)] (ca. 10%) being observed by ¹¹B NMR spectroscopy (Scheme 8a, Figure S34). The cyclic diborazane, [Me₂N-BHMe]₂, was observed by ¹¹B NMR spectroscopy as two doublet peaks, consistent with the presence of *cis* and *trans* isomers.

The reaction of the sterically encumbered *B*-methylated amine-borane **1d** with 2.5 mol % [Rh(COD)(μ-Cl)]₂ (5 mol % Rh) in THF at 20 °C was observed to be substantially slower than for **1a**–**1c**, with complete consumption of **1d** requiring 120 h. The products detected by ¹¹B NMR spectroscopy were *i*Pr₂N=BHMe (ca. 80%), and the presumed, dehydrogenated

Scheme 8. Catalytic Dehydrocoupling of (a) **1c** and (b) **1d** in THF at 20 °C ([M] = 2.5 mol % [Rh(COD)(μ-Cl)]₂, 5 mol % IrH₂(POCOP), 10 mol % Skeletal Nickel)^a

^aSpecies that appear with only specific substrates and precatalysts are labeled as follows: (red) with **1c** and [Rh(COD)(μ-Cl)]₂ or skeletal nickel, (blue) with **1d** and [Rh(COD)(μ-Cl)]₂ or skeletal nickel, (purple) with **1d** and [Rh(COD)(μ-Cl)]₂.

redistribution product *i*Pr₂N=BMe₂ (ca. 20%) (Scheme 8b, Figure S35).

2.3.2. Catalytic Dehydrocoupling of 1a–1d with IrH₂(POCOP) and Skeletal Nickel. Similar to the dehydrocoupling of **1a** with [Rh(COD)(μ-Cl)]₂, the reaction of **1a** with 5 mol % IrH₂(POCOP) in THF at 20 °C required 1 h for complete consumption of amine-borane and yielded [NH-BMe]₃ (ca. 90%). However, *B*-methylbis(amino)borane (NH₂)₂BMe [$\delta_{\text{B,exp}}$ 32.1 (s)] [$\delta_{\text{B,calc}}$ 31.0] (ca. 10%) was also detected as a second product by ¹¹B NMR spectroscopy (Scheme 7a, Figure S36). In contrast, the reaction of **1a** with 10 mol % skeletal nickel in THF at 20 °C was significantly slower than for both [Rh(COD)(μ-Cl)]₂ and IrH₂(POCOP) as precatalysts, with complete consumption of **1a** detected after 24 h together with the formation of the same two products as for IrH₂(POCOP), namely borazine [NH-BMe]₃ (ca. 80%) and (NH₂)₂BMe (ca. 20%) (Scheme 7a, Figure S37).

In contrast to the results for **1a**, a significantly faster reaction was observed for **1b** with 5 mol % IrH₂(POCOP) than for [Rh(COD)(μ-Cl)]₂ in THF at 20 °C, with complete consumption of the amine-borane observed after 1 h rather than 24 h. However, a more complex array of products was formed, including *B*-methyl-*N*-methyl aminoborane, MeNH=BHMe [$\delta_{\text{B,exp}}$ 41.9 (d, ¹J_{BH} = 116 Hz)] [$\delta_{\text{B,calc}}$ 44.0 (¹J_{BH} = 122 Hz)] (ca. 20%), cyclic *B*-methyl-*N*-methyl diborazane [MeNH-BHMe]₂ [$\delta_{\text{B,exp}}$ 1.4 (d, ¹J_{BH} = 114 Hz)] [$\delta_{\text{B,calc}}$ -0.8 (¹J_{BH} = 111 Hz)] (ca. 20%), and [MeN-BMe]₃ (ca. 60%) (Scheme 7b, Figure S38). Not only was the reaction of **1b** with 10 mol % skeletal nickel in THF at 20 °C slower than that for IrH₂(POCOP) (24 h), a wider range of products was formed, including MeNH=BHMe (ca. 10%), MeNH=BMe₂ (ca. 10%), [MeNH-BHMe]₂ (ca. 30%), [MeN-BMe]₃ (ca. 20%), and (MeNH)₂BMe (ca. 30%) (Scheme 7b, Figure S39).

As with the case of [Rh(COD)(μ-Cl)]₂ as a precatalyst, the reaction of **1c** with 5 mol % IrH₂(POCOP) in THF at 20 °C was complete after 24 h. Moreover, in contrast to the formation of an array of products as in the former case, only two products were present by ¹¹B NMR spectroscopy: Me₂N=BHMe (ca. 60%) and [Me₂N-BHMe]₂ (ca. 40%) (Scheme 8a, Figure S40). Similarly, complete consumption of **1c** was observed by ¹¹B NMR spectroscopy after 24 h with 10 mol % skeletal nickel in THF at 20 °C, with the formation of Me₂N=BHMe (ca.

40%), $[\text{Me}_2\text{N}-\text{BHMe}]_2$ (ca. 30%), $(\text{Me}_2\text{N})_2\text{BMe}$ (ca. 10%), and an unassigned product $[\delta_{\text{B,exp}} 0.9 \text{ (m)}]$ (ca. 20%) (Scheme 8a, Figure S41).

No reaction was observed following the attempted dehydrogenation of **1d** with 5 mol % $\text{IrH}_2(\text{POCOP})$ in THF at 20 °C after 120 h by ^{11}B NMR spectroscopy (Figure S42). In contrast, **1d** underwent dehydrogenation to yield the aminoborane, $i\text{Pr}_2\text{N}=\text{BHMe}$, as the sole product, using 10 mol % skeletal nickel in THF at 20 °C, as observed by ^{11}B NMR spectroscopy. Nevertheless, the reaction proceeded significantly slower compared to the reaction of **1d** with $[\text{Rh}(\text{COD})(\mu\text{-Cl})]_2$ as a precatalyst, with 70% conversion being observed after 210 h (Scheme 8b, Figure S43).

2.4. Attempted Dehydropolymerization of 1a and 1b with Skeletal Nickel. We have previously prepared high molecular weight poly(*N*-methyl aminoborane), $[\text{MeNH}-\text{BH}_2]_n$, using stoichiometric amounts of skeletal nickel via the dehydropolymerization of $\text{MeNH}_2\cdot\text{BH}_3$.^{6a} We explored analogous reactions of **1a** and **1b** in an attempt to prepare the currently unknown B-methylated polyaminoborane, $[\text{NHR}-\text{BHMe}]_n$ ($\text{R} = \text{H}$ or Me).

First, **1a** was treated with 100 mol % skeletal nickel in THF at 20 °C and the reaction was monitored by ^{11}B NMR spectroscopy. After 1 h, ca. 40% conversion of **1a** to borazine $[\text{NH}-\text{BMe}]_3$ (ca. 20%) and $(\text{NH}_2)_2\text{BMe}$ (ca. 10%) was observed and, in addition, a broad peak that was tentatively assigned to be oligo/poly(*B*-methyl aminoborane) $[\text{NH}_2-\text{BHMe}]_x$ $[\delta_{\text{B,exp}} -7.8$ to $-9.1 \text{ (br)}]$ ³⁵ (ca. 10%) (Scheme 9a,

Scheme 9. Attempted Dehydropolymerization of (a) 1a and (b) 1b with Stoichiometric Amounts of Skeletal Nickel in THF at 20 °C

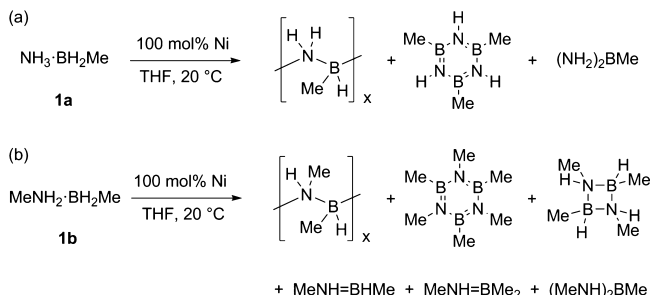


Figure S44). After allowing the reaction to continue for 24 h, both **1a** and the tentatively assigned $[\text{NH}_2-\text{BHMe}]_x$ were no longer detected, with $[\text{NH}-\text{BMe}]_3$ (ca. 90%) and $(\text{NH}_2)_2\text{BMe}$ (ca. 10%) being the only products observed (Figure S45). These results suggest that, if oligo/poly(*B*-methyl aminoborane) is indeed formed, this material undergoes dehydrogenation and depolymerization much more readily than the *N*-methyl analogue, $[\text{MeNH}-\text{BH}_2]_n$.³⁶

Next, we explored the analogous reaction of **1b** with 100 mol % skeletal nickel in THF at 20 °C. After 1 h, 80% conversion was observed by ^{11}B NMR spectroscopy with the formation of $\text{MeNH}=\text{BHMe}$ (ca. 10%) and $[\text{MeNH}-\text{BHMe}]_2$ (ca. 20%) along with unidentified products $[\delta_{\text{B,exp}} 40.8 \text{ (s)}]$ (ca. 10%), $[\delta_{\text{B,exp}} 2.2 \text{ (s)}]$ (ca. 10%), $[\delta_{\text{B,exp}} -0.2 \text{ (d)}]$ (ca. 20%), and $[\delta_{\text{B,exp}} -2.6 \text{ (br)}]$ (ca. 10%) (Scheme 9b, Figure S46). The peaks detected between δ_{B} 2.2 and -2.6 ppm were tentatively assigned to oligo/poly(*B*-methyl-*N*-methyl aminoborane), $[\text{MeNH}-\text{BHMe}]_x$.³⁵ After 24 h, the ^{11}B NMR spectrum indicated that **1b**, $\text{MeNH}=\text{BHMe}$, $[\text{MeNH}-\text{BHMe}]_2$, and the

tentatively assigned oligomeric/polymeric species had been consumed. The only products detected were $[\text{MeN}-\text{BMe}]_3$ (ca. 90%), $\text{MeNH}=\text{BMe}_2$ (ca. 5%), and $(\text{MeNH})_2\text{BMe}$ (ca. 5%) (Figure S47). Again, it appears that any oligo/poly(*B*-methyl-*N*-methyl aminoborane) formed readily undergoes further dehydrogenation and depolymerization under the reaction conditions.

2.5. Hydrogen Transfer Reactions of 1a–1d with $i\text{Pr}_2\text{N}=\text{BH}_2$. Following previous work from our group on hydrogen transfer from amine-boranes to *N*-diisopropyl aminoborane, $i\text{Pr}_2\text{N}=\text{BH}_2$,^{1ij} the ability for B-methylated amine-boranes **1a–1d** to act as hydrogen donors was investigated. Thus, a stoichiometric amount of $i\text{Pr}_2\text{N}=\text{BH}_2$ (in THF) was added to solid **1a** at 20 °C and monitored by ^{11}B NMR spectroscopy. After 10 min, complete hydrogenation of $i\text{Pr}_2\text{N}=\text{BH}_2$ to $i\text{Pr}_2\text{NH}\cdot\text{BH}_3$ was observed, along with the formation of borazine $[\text{NH}-\text{BMe}]_3$ and oligo/polyaminoborane $[\text{NH}_2-\text{BHMe}]_{2,3,\text{or } x}$ ³⁵ products expected from dehydrogenation/oligomerization of $\text{NH}_2=\text{BHMe}$ (Scheme 10a,

Scheme 10. Hydrogen Transfer of (a) 1a with $i\text{Pr}_2\text{N}=\text{BH}_2$ in THF at 20 °C and (b) 1a with $i\text{Pr}_2\text{N}=\text{BH}_2$ in THF at 20 °C in the Presence of Two Equivalents of Cyclohexene ($\text{Cy} = \text{C}_6\text{H}_{11}$)

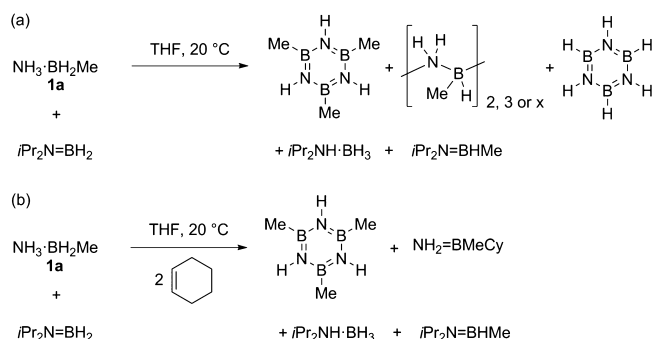


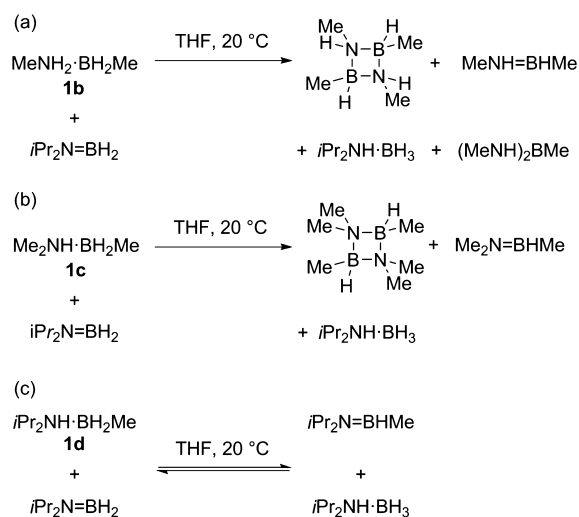
Figure S48). No substantial change in the reaction mixture was detected by ^{11}B NMR spectroscopy after 1 h (Figure S49). However, each set of ^{11}B and $^{11}\text{B}\{^1\text{H}\}$ NMR spectra also showed the presence of several other peaks, of which some could not be successfully assigned. Nonetheless, one very minor product, generally detected at a level corresponding to ca. 1%, was identified as $i\text{Pr}_2\text{N}=\text{BHMe}$ $[\delta_{\text{B,exp}} 39.6 \text{ (d, } ^1J_{\text{BH}} = 122 \text{ Hz)}]$, the major dehydrogenation product formed in the catalytic dehydrogenation of **1d** with Rh and Ni precatalysts (see section 2.3). The formation of this species was surprising as it represents a cross-product where the methyl substituent on boron presumably arises from the amine-borane substrate, **1a**. Another unexpected product was identified as borazine, $[\text{NH}-\text{BH}]_3$ $[\delta_{\text{B,exp}} = 29.4 \text{ (d, } ^1J_{\text{BH}} = 141 \text{ Hz)}]$ $[\delta_{\text{B,lit}} = 30.2 \text{ (d, } ^1J_{\text{BH}} = 141 \text{ Hz)}]$.^{4a}

Transient aminoboranes that exist sufficiently long in solution can be trapped through hydroboration with cyclohexene to yield, for the case of $\text{NH}_2=\text{BH}_2$, *B*-dicyclohexyl aminoborane, $\text{NH}_2=\text{BCy}_2$ ($\text{Cy} = \text{C}_6\text{H}_{11}$).^{1i,37} To investigate whether hydrogen transfer between **1a** and $i\text{Pr}_2\text{N}=\text{BH}_2$ occurs via formation of a transient aminoborane, $\text{NH}_2=\text{BHMe}$, amine-borane **1a** was added to one equivalent of $i\text{Pr}_2\text{N}=\text{BH}_2$ and two equivalents of cyclohexene in THF at 20 °C, and the subsequent reaction was monitored by ^{11}B NMR spectroscopy. After 1 h, hydrogenation of $i\text{Pr}_2\text{N}=\text{BH}_2$ to $i\text{Pr}_2\text{NH}\cdot\text{BH}_3$ was observed, together with the formation of the hydroborated

aminoborane species, *B*-methylcyclohexyl aminoborane, $\text{NH}_2=\text{BMeCy}$ [$\delta_{\text{B,exp}}$ 46.7 (s)] [$\delta_{\text{B,calc}}$ 49.2] (Scheme 10b, Figure S50). Consistent with these results, the interception of $\text{NH}_2=\text{BHMe}$ by cyclohexene almost completely prevents the formation of the oligomer, $[\text{NH}_2-\text{BHMe}]_x$.

As with the case of **1a** as a hydrogen donor, a stoichiometric amount of $i\text{Pr}_2\text{N}=\text{BH}_2$ (in THF) was added to solid **1b** at 20 °C. The reaction was monitored by ^{11}B NMR spectroscopy with 90% hydrogenation of $i\text{Pr}_2\text{N}=\text{BH}_2$ to $i\text{Pr}_2\text{NH}\cdot\text{BH}_3$ detected after 10 min and subsequent formation of $\text{MeNH}=\text{BHMe}$, $[\text{MeNH}-\text{BHMe}]_2$, and $(\text{MeNH})_2\text{BMe}$ (Scheme 11a, Figure S51). No further reaction was detected by ^{11}B NMR spectroscopy after 1 h (Figure S52).

Scheme 11. Hydrogen Transfer of (a) **1b**, (b) **1c**, and (c) **1d** with $i\text{Pr}_2\text{N}=\text{BH}_2$ in THF at 20 °C



Similar to the case of the hydrogen transfer reaction between **1a** and $i\text{Pr}_2\text{N}=\text{BH}_2$, trapping of the likely transient monomeric aminoborane intermediate, in this instance, $\text{MeNH}=\text{BHMe}$, was attempted with cyclohexene. Under analogous conditions, **1b** was added to one equivalent of $i\text{Pr}_2\text{N}=\text{BH}_2$ and two equivalents of cyclohexene in THF at 20 °C. After 1 h, hydrogenation of $i\text{Pr}_2\text{N}=\text{BH}_2$ to $i\text{Pr}_2\text{NH}\cdot\text{BH}_3$ was detected, along with the formation of $[\text{MeNH}-\text{BHMe}]_2$ and a peak at $\delta_{\text{B,exp}}$ 45.4 (s), assigned to $\text{MeNH}=\text{BMeCy}$ [$\delta_{\text{B,calc}}$ 47.3], as well as minor amounts of $\text{MeNH}=\text{BHMe}$ by ^{11}B NMR spectroscopy (Figure S53).

Slower hydrogen transfer was detected between **1c** and $i\text{Pr}_2\text{N}=\text{BH}_2$, with 45% hydrogenation after 10 min in THF at 20 °C by ^{11}B NMR spectroscopy. As well as the formation of $i\text{Pr}_2\text{NH}\cdot\text{BH}_3$, the dehydrogenated product $\text{Me}_2\text{N}=\text{BHMe}$ was also detected (Scheme 11b, Figure S54). After 1 h, further hydrogenation (72%) was observed as well as the appearance of the cyclic diborazane, $[\text{Me}_2\text{N}-\text{BHMe}]_2$ (Figure S55). In the case of **1c**, the presence of cyclohexene resulted in no new products corresponding to the trapped aminoborane, $\text{Me}_2\text{N}=\text{BMeCy}$, being observed for the reaction of **1c** with one

equivalent of $i\text{Pr}_2\text{N}=\text{BH}_2$ and two equivalents of cyclohexene in THF at 20 °C after 1 h by ^{11}B NMR spectroscopy (Figure S56).

In contrast to the very rapid (**1a** and **1b**) and slower (**1c**) hydrogen transfer between **1a–1c** and $i\text{Pr}_2\text{N}=\text{BH}_2$, no reaction was observed between a stoichiometric amount of $i\text{Pr}_2\text{N}=\text{BH}_2$ and the sterically encumbered *B*-methylated amine-borane, **1d**, in THF at 20 °C after 1 h (Figure S57). However, after 24 h, a small amount of hydrogen transfer was detected, as shown by ^{11}B NMR spectroscopy with hydrogenation of $i\text{Pr}_2\text{N}=\text{BH}_2$ to $i\text{Pr}_2\text{NH}\cdot\text{BH}_3$ and concomitant dehydrogenation of **1d** to $i\text{Pr}_2\text{N}=\text{BHMe}$ (Scheme 11c, Figure S58). The reaction progressed until an apparent equilibrium was established^{1j} after 56 days with 95% hydrogenation of $i\text{Pr}_2\text{N}=\text{BH}_2$ (Figure S59).

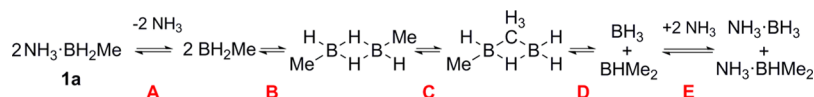
3. DISCUSSION

3.1. Thermally Induced Redistribution and Dehydrogenation Reactions of 1a–1d. The *B*-methylated amine-borane, **1a**, was observed to undergo methyl and hydrogen redistribution at boron at ambient (20 °C, in toluene) and elevated (70 °C, in toluene or THF) temperatures that resulted in the formation of $\text{NH}_3\cdot\text{BMe}_3$, $\text{NH}_3\cdot\text{BHMe}_2$, and $\text{NH}_3\cdot\text{BH}_3$ (see section 2.2, Schemes 4 and 5).

The redistribution of substituents at boron in three-coordinate boranes is well-known, and the mechanism has been proposed to occur via a diborane intermediate.³⁸ However, limited research has involved studies of analogous four-coordinate boron species,³⁹ with no reports of redistribution of alkyl substituents at boron as part of an amine-borane.⁴⁰ Benton and Miller investigated the reaction between two amine-boranes with different halogen substituents at boron (selected from $\text{Me}_3\text{N}\cdot\text{BX}_3$ (X = F, Cl, Br, I)) and reported that when the solution was heated at 50 °C (CH_2Cl_2), 70 °C (CHCl_3), and 100 °C ($\text{C}_6\text{H}_5\text{Cl}$) for 6 h, no redistribution was observed.⁴¹ However, when the reaction was heated to 160 °C in the gas phase, redistribution of the halogen substituents was noted. In addition, labeling studies where one of the amine-boranes was ^{10}B enriched (and the other consisted of natural abundance boron, ca. 80% ^{11}B , ca. 20% ^{10}B) showed evidence for redistribution of ^{10}B between the amine-borane substrates, suggesting redistribution occurred via B–N bond cleavage.

In a similar manner to that suggested by Benton and Miller for *B*-halogenated amine-boranes,⁴¹ the redistribution of the methyl and hydrogen substituents at boron for *B*-methylated amine-boranes was postulated to arise through dissociation of the B–N bond to yield free amine and borane (Scheme 12, step A). Subsequent dimerization of two electron deficient borane molecules would lead to a diborane intermediate (Scheme 12, step B). Redistribution of methyl and hydrogen at boron could be rationalized by cleavage and formation of a bond between boron and the bridging moiety (Scheme 12, step C). Retrodimerization of a hydrogen–methyl-bridged diborane would yield two boranes (Scheme 12, step D) that reassociate with free amine to reform two different amine-boranes (Scheme 12, step E). In principle, this process could be

Scheme 12. Postulated Mechanism of the Methyl–Hydrogen Exchange Reaction of **1a**



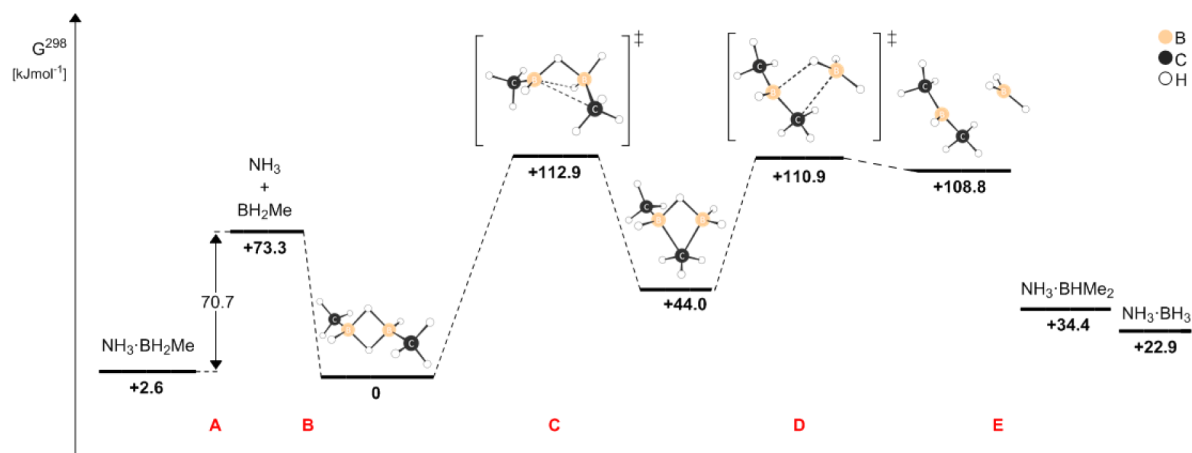


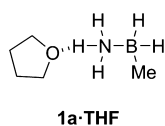
Figure 4. Calculated relative Gibbs free energies G^{298} (in kJ mol^{-1}) for the methyl–hydrogen exchange reaction of **1a**. Calculations were performed at the M06-2X/cc-pVTZ level of theory; solvent corrections for THF were applied.²⁵

repeated to yield the full range of possible amine-boranes with different combinations of methyl and hydrogen substituents at boron.

This proposed mechanism was probed by DFT calculations as a THF solution with the dissociation energy of the B–N bond of **1a** calculated to be $+70.7 \text{ kJ mol}^{-1}$ (Figure 4, step A). The diborane, formed from two BH_2Me moieties (Figure 4, step B), can be bridged by either two hydrogen atoms or a hydrogen atom and a methyl group ($+44.0 \text{ kJ mol}^{-1}$ relative to the dihydrogen-bridged diborane). A dimethyl-bridged diborane was also considered to be a possible intermediate, but as expected, the corresponding calculated energy was considerably higher ($+114.9 \text{ kJ mol}^{-1}$), implying that the species is unlikely to be formed during the redistribution reaction. The activation energy associated with the interconversion of the dihydrogen-bridged and hydrogen–methyl-bridged diborane intermediates, where cleavage of a B–H bridge bond and rotation of one BH_2Me moiety around the remaining B–H bond occurs to lead to the formation a new B–C bridging bond, was calculated to be $+112.9 \text{ kJ mol}^{-1}$ (Figure 4, step C). The energy for the retrodimerization of the diborane to two boranes was determined to be $+66.9 \text{ kJ mol}^{-1}$ (Figure 4, step D), with an exergonic reassociation of ammonia with the free boranes to form amine-boranes, $\text{NH}_3\cdot\text{BH}_3$ ($-85.9 \text{ kJ mol}^{-1}$) and $\text{NH}_3\cdot\text{BHMe}_2$ ($-74.4 \text{ kJ mol}^{-1}$) (Figure 4, step E).

Redistribution of methyl and hydrogen substituents at boron was observed for **1a** in toluene but not in THF at 20°C . Based on previous observations of oxygen-containing species coordinating to the protic hydrogen on nitrogen in amine-boranes and their dehydrocoupling products,^{29a,43} a possible explanation involves stabilization of the amine-borane via hydrogen bonding to the donating THF solvent (Scheme 13). However, DFT calculations determined that **1a**·THF was higher in energy than the corresponding dihydrogen-bridged diborane (formed in step B in Figure 4) by $+19.5 \text{ kJ mol}^{-1}$ and similar ^{11}B NMR chemical shifts for **1a** in THF ($\delta_{\text{B,exp}} = -16.3$)

Scheme 13. Structure of Postulated THF Stabilized B-Methyl Amine-Borane (**1a**·THF)



and toluene ($\delta_{\text{B,exp}} = -15.7$) suggests that such an effect, if it exists, has only a small effect on the B–N bond strength. The B-methylated amine-boranes **1a–1d** were also calculated to be slightly more stable as a solution in THF than in toluene, by $8.0\text{--}13.8 \text{ kJ mol}^{-1}$ (Table S5).²⁵ As a more polar solvent, THF probably provides a solution environment in which the amine-borane with polar N–H and B–H bonds is more stable, thereby providing a possible explanation why redistribution was not observed for **1a** in THF at 20°C .

Redistribution of methyl and hydrogen substituents in the B-methylated amine-boranes **1b–1d** was not detected in toluene at 20°C after 170 h, but scrambling was observed at 70°C , with a rate for complete consumption of the amine-borane in the order **1b** > **1c** > **1d** (see section 2.2.2). The electron donating alkyl groups at nitrogen would be expected to strengthen the dative bond between the nitrogen and boron, resulting in an increased resistance to dissociation. This was supported by DFT calculations for **1b** and **1c**, where the bond dissociation energies in toluene increased from $+124.9 \text{ kJ mol}^{-1}$ for **1a** to $+142.9$ and $+150.5 \text{ kJ mol}^{-1}$ for **1b** and **1c**, respectively (Table 4). However, the bond dissociation energy

Table 4. Amount of Time Required for Complete Consumption of B-Methylated Amine-Boranes **1a–1d** in Toluene at 70°C and Calculated Bond Dissociation Energies (D_0) of **1a–1d**^a

amine-borane	time required for complete consumption of 1a–1d in toluene at $70^\circ\text{C}/\text{h}$ ^b	calcd D_0 of B–N bond/ kJ mol^{-1}
1a	24	$+124.9$
1b	48	$+142.9$
1c	170	$+150.5$
1d	500	$+128.7$

^aCalculations were performed at the M06-2X/cc-pVTZ level of theory; solvent corrections for toluene were applied.²⁵ ^bBased on ^{11}B NMR spectroscopy.

for **1d** ($+128.7 \text{ kJ mol}^{-1}$) was calculated to be close to that for **1a**. This was not unexpected as the B–N bond length for **1d** determined by X-ray diffraction was elongated compared to **1a** and **1b** (Table 2), where the steric effect of the isopropyl groups on nitrogen appeared to have a greater influence on the bond distance than their electron donating characteristic. The much lower reactivity of **1d** toward redistribution despite the

Table 5. Comparison of Percentage Hydrogenation of $i\text{Pr}_2\text{N}=\text{BH}_2$ to $i\text{Pr}_2\text{NH}\cdot\text{BH}_3$ Using Hydrogen Donating Amine-Boranes **1a–1c** and $\text{RR}'\text{NH}\cdot\text{BH}_3$ ($\text{R}, \text{R}' = \text{H}, \text{Me}$) in THF at 20 °C^a

amine-borane	hydrogenation of $i\text{Pr}_2\text{N}=\text{BH}_2/\%$ ⁴⁵		$\Delta G^{\ddagger b}/\text{kJ mol}^{-1}$	$\Delta G^{298c}/\text{kJ mol}^{-1}$	ref
	after 10 min	after 1 h			
$\text{NH}_3\cdot\text{BH}_3$	89	98	—	—	45
1a	100	100	+64.7	−23.6	this work
$\text{MeNH}_2\cdot\text{BH}_3$	56	91	—	—	45
1b	90	92	+74.1	−20.0	this work
$\text{Me}_2\text{NH}\cdot\text{BH}_3$	4	16	+86.9	+9.1	1j
1c	45	72	+76.0	−14.7	this work

^aCalculations performed at the M06-2X/cc-pVTZ level of theory; solvent corrections for THF were applied.²⁵ ^bActivation energy of hydrogen transfer. ^cGibbs free energy of hydrogen transfer.

apparently weaker B–N bond was likely a consequence of the unfavorable formation of the redistribution products, $i\text{Pr}_2\text{NH}\cdot\text{BHMe}_2$ and $i\text{Pr}_2\text{NH}\cdot\text{BMe}_3$, on steric grounds. Indeed, neither species was detected on thermolysis at 70 °C after 500 h. Instead, the exclusive formation of their dehydrogenated derivatives $i\text{Pr}_2\text{N}=\text{BMe}_2$ and $i\text{Pr}_2\text{N}=\text{BHMe}$ was evidenced, together with $i\text{Pr}_2\text{NH}\cdot\text{BH}_3$ (Figure S28). This suggests that, in the case of **1d**, the reaction was driven by the subsequent dehydrogenation of the initially formed, sterically disfavored redistribution products and the very slow amine-borane consumption rate was a likely consequence.

3.2. Catalytic Dehydrocoupling Reactions of **1a–1d**.

The reactivity of the B-methylated amine-boranes **1a–1d** with respect to catalytic dehydrocoupling/dehydrogenation varied significantly (see section 2.3). As previously noted, DFT calculations highlight that the inclusion of a methyl group at boron energetically favors dehydrogenation.¹⁹ Favorable kinetics were also apparent, with shorter reaction times being observed for B-methylated amine-borane dehydrocoupling/dehydrogenation, compared to analogous amine-boranes without a methyl group at boron. For example, treatment of **1a** with 2.5 mol % $[\text{Rh}(\text{COD})(\mu\text{-Cl})_2]$ precatalyst for 1 h in THF led to the release of two equivalents of hydrogen to form the borazine $[\text{NH}-\text{BMe}]_3$ quantitatively at ambient temperature by ¹¹B NMR spectroscopy. In comparison, the catalytic dehydrocoupling of $\text{MeNH}_2\cdot\text{BH}_3$ with the same precatalyst yielded *N*-trimethyl borazine, $[\text{MeN}-\text{BH}]_3$, but elevated temperatures (45 °C) and an extended reaction time (ca. 48–84 h) were required.^{4a}

We have previously reported that $\text{IrH}_2(\text{POCOP})$ functions as an efficient dehydropolymerization catalyst for $\text{MeNH}_2\cdot\text{BH}_3$ to form high molecular weight poly(*N*-methyl aminoborane), $[\text{MeNH}-\text{BH}_2]_n$, in THF at 20 °C within 20 min.^{5c} However, treatment of **1a** and **1b** with 5 mol % $\text{IrH}_2(\text{POCOP})$ resulted in two equivalents of hydrogen being released to yield borazine products, $[\text{RN}-\text{BMe}]_3$ ($\text{R} = \text{H}, \text{Me}$). No reaction was observed for **1d** with a catalytic amount of the iridium complex, which is presumably the result of both the precatalyst and substrate being too sterically encumbered for a catalytic reaction to take place. Successful dehydrocoupling was observed for **1c** in THF at 20 °C within 24 h, a surprising result in comparison to the analogous amine-borane without a methyl substituent at boron, $\text{Me}_2\text{NH}\cdot\text{BH}_3$, which was reported to undergo very slow catalytic dehydrocoupling, with less than one equivalent of hydrogen being released after 48 h in THF at 25 °C.^{5b} Similar to the case of $[\text{Rh}(\text{COD})(\mu\text{-Cl})_2]$ as a precatalyst, the increased reactivity of $\text{IrH}_2(\text{POCOP})$ toward B-methylated amine-boranes **1a–1c** compared to the *N*-methyl analogues was postulated to be due to the favorable dehydrocoupling/

dehydrogenation kinetics and thermodynamics arising from the presence of the electron donating methyl group at boron.

The use of catalytic amounts of skeletal nickel resulted in successful dehydrocoupling of all the B-methylated amine-boranes **1a–1d** but with reduced selectivity. Since **1d** only reached ca. 70% conversion after 120 h, poisoning of the nickel surface was postulated to occur before complete conversion of **1d** to $i\text{Pr}_2\text{N}=\text{BHMe}$ was achieved. The poisoning of heterogeneous catalysts by species with B–H bonds has been demonstrated by our group in the case of Rh colloids.⁴⁴ Based on the previous results, boranes arising from dissociation of the B-methylated amine-borane adducts likely lead to hydrogen gas release and concomitantly form a boron-containing layer on the nickel surface, rendering the catalyst inactive.

3.3. Attempted Dehydropolymerization of **1a and **1b** with Skeletal Nickel.** Our group has previously reported the reaction of $\text{MeNH}_2\cdot\text{BH}_3$ with a stoichiometric amount of skeletal nickel, whereby after 2 h in THF at 20 °C high molecular weight poly(*N*-methyl aminoborane) was isolated with 60% yield.^{6a} With the aim of isolating the first high molecular weight polyaminoborane with non-hydrogen substituents at boron, the amine-boranes **1a** and **1b** were therefore also treated with a stoichiometric amount of skeletal nickel in THF at 20 °C. In the case of **1a**, partial consumption of the amine-borane after 1 h was detected, together with the presence of the tentatively assigned oligomer/polymer, $[\text{NH}_2-\text{BHMe}]_n$, observed as a broad peak between −7.8 and −9.1 ppm by ¹¹B NMR spectroscopy. However, after 24 h, both the tentatively assigned oligomer/polymer and the B-methylated amine-borane were no longer detectable and the final products were borazine, $[\text{NH}-\text{BMe}]_3$, and bis(amino)-borane $(\text{NH}_2)_2\text{BMe}$. A similar observation was noted for the reaction of **1b** with 100 mol % skeletal nickel in THF at 20 °C. The methyl group at boron presumably increases the hydridic nature of the hydrogen cosubstituents at boron, favoring further dehydrogenation of oligo/poly(*B*-methyl aminoborane) to borazine. Thus, the oligomer/polymer was only observed as an intermediate before undergoing further dehydrocoupling to the more thermodynamically favorable borazine.

3.4. Hydrogen Transfer Reactions of **1a–1d with $i\text{Pr}_2\text{N}=\text{BH}_2$.** Hydrogen transfer was detected between B-methylated amine-boranes **1a–1d** and $i\text{Pr}_2\text{N}=\text{BH}_2$ in THF at 20 °C, although the reaction progressed dramatically slower in the case of **1d**. To compare the hydrogen donating abilities of **1a–1c** to amine-boranes without a methyl group at boron, the percentage hydrogenation of $i\text{Pr}_2\text{N}=\text{BH}_2$ to $i\text{Pr}_2\text{NH}\cdot\text{BH}_3$ was determined after 10 min and 1 h by relative integration in the ¹¹B NMR spectra (Table 5).^{1j,45} After 10 min, at least 90% hydrogenation of $i\text{Pr}_2\text{N}=\text{BH}_2$ to $i\text{Pr}_2\text{NH}\cdot\text{BH}_3$ was detected

using **1a** and **1b** as hydrogen donors. For amine-boranes without a methyl group at boron, the percentage hydrogenation decreased significantly from 89% (for $\text{NH}_3\cdot\text{BH}_3$) to 4% (for $\text{Me}_2\text{NH}\cdot\text{BH}_3$) after 10 min. In comparison, for analogous amine-boranes with a methyl group at boron, larger values and a less substantial decrease were observed from 100% (for **1a**) to 45% (for **1c**).

Although **1d** undergoes hydrogen transfer with $i\text{Pr}_2\text{N}=\text{BH}_2$ at a markedly slower rate than for **1a–1c**, subsequent reactivity of the resulting aminoborane $i\text{Pr}_2\text{N}=\text{BHMe}$ was not observed, with only this species and $i\text{Pr}_2\text{NH}\cdot\text{BH}_3$ being detected as products by ^{11}B NMR spectroscopy (Scheme 11c). This system reached an apparent equilibrium after 56 days with the percentage hydrogenation of $i\text{Pr}_2\text{N}=\text{BH}_2$ determined to be ca. 95%. Interestingly, although this equilibrium required a significantly longer time to establish, the percentage hydrogenation was substantially greater when compared to that for the reaction of $\text{Me}_2\text{NH}\cdot\text{BH}_3$ with $i\text{Pr}_2\text{N}=\text{BH}_2$ (54%), which required 18 h in THF at 20 °C.^{11j} This suggests that, although the sterically encumbered nature of **1d** results in a slow reaction, the favorable thermodynamics enables the reaction to reach near completion.

The increased hydrogen donating ability observed for **1a–1d** toward $i\text{Pr}_2\text{N}=\text{BH}_2$ is presumably a consequence of the presence of the electron donating methyl group at boron. The enhanced hydridic character of the hydrogen substituents at boron would be expected to lead to faster dehydrogenation reactions. The hydrogen transfer from **1a–1d** also appears to be thermodynamically more favorable, which is in agreement with the previous work by Dixon and co-workers where dehydrogenation was calculated to be more exergonic as the number of methyl substituents at boron increased.¹⁹

To further probe the mechanism of hydrogen transfer, DFT studies were conducted for **1a–1c** with $i\text{Pr}_2\text{N}=\text{BH}_2$ (Figure 5,

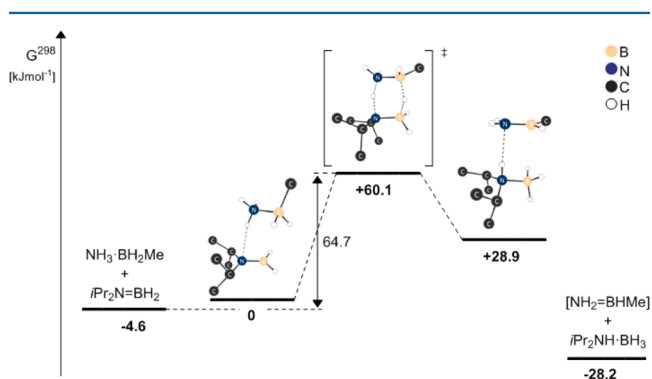


Figure 5. Calculated relative Gibbs free energies G^{298} (in kJ mol^{-1}) for the hydrogen transfer reaction of **1a** with $i\text{Pr}_2\text{N}=\text{BH}_2$. Calculations performed at the M06-2X/cc-pVTZ level of theory; solvent corrections for THF were applied.²⁵ All hydrogen atoms bonded to carbon were omitted for clarity.

Figures S65 and S66).²⁵ In each case, a concerted mechanism with a transition state of a six-membered ring was determined, indicating that both hydrogen atoms were transferred in the same step. An analogous transition state was identified for the hydrogen transfer reaction of $\text{Me}_2\text{NH}\cdot\text{BH}_3$ with $i\text{Pr}_2\text{N}=\text{BH}_2$.^{1j}

In our previously investigated reaction of $\text{Me}_2\text{NH}\cdot\text{BH}_3$ with $i\text{Pr}_2\text{N}=\text{BH}_2$, the activation energy associated with the formation of the six-membered cyclic transition state was found to be $+86.9 \text{ kJ mol}^{-1}$,⁴⁶ which was higher than that

calculated for **1a–1c** ($+64.7$ to $+76.0 \text{ kJ mol}^{-1}$) (Table S). Hydrogen transfer from $\text{Me}_2\text{NH}\cdot\text{BH}_3$ to $i\text{Pr}_2\text{N}=\text{BH}_2$ was reported to be slightly endergonic ($+9.1 \text{ kJ mol}^{-1}$), in contrast to the Gibbs free energies determined for **1a–1c**, which were exergonic (-14.7 to $-23.6 \text{ kJ mol}^{-1}$). Prior and subsequent to the formation of the cyclic transition state, encounter complexes were located, which were attributed to the presence of the cyclic hydrogen bonding. Although these complexes were determined to be slightly endergonic compared to initial and final products, the activation energy was effectively reduced, further favoring the hydrogen transfer reaction. This shows that, both kinetically and thermodynamically, B-methylated amine-boranes **1a–1c** have an improved ability to function as hydrogen donors toward the aminoborane $i\text{Pr}_2\text{N}=\text{BH}_2$ than $\text{Me}_2\text{NH}\cdot\text{BH}_3$.

The hydrogen transfer reaction of **1a** with $i\text{Pr}_2\text{N}=\text{BH}_2$ resulted in the detection of very small quantities of the unexpected product, $i\text{Pr}_2\text{N}=\text{BHMe}$, with substituents apparently derived from each of the reactants. In addition, the borazine $[\text{NH}=\text{BH}]_3$, with no methyl groups at boron, was also formed as another surprising product. The mechanism of formation for these species is unclear,⁴⁷ and is the subject of ongoing studies.

4. SUMMARY

Detailed studies of the reactivity of a series of B-methylated amine-boranes with different substituents (H, Me, *i*Pr) at nitrogen have revealed a range of interesting, unexpected, complex, and potentially useful chemistry. First, redistribution of methyl and hydrogen substituents at boron was observed in solution at ambient and elevated temperatures. This was proposed to arise from dissociation of the amine-borane adduct with subsequent redistribution of the substituents in the borane via formation of a diborane intermediate. To our knowledge, this represents the first demonstration of redistribution reactions at a four-coordinate boron center under mild conditions.

Rapid dehydrocoupling of B-methylated amine-boranes with Rh(I), Ir(III), and Ni(0) precatalysts was detected to yield a variety of products including aminoboranes, cyclic diborazanes, and borazines, based on in situ ^{11}B NMR spectroscopy with peak assignments supported by DFT calculations. In comparison to the well-studied catalytic dehydrocoupling of N-methylated amine-boranes, faster dehydrocoupling/dehydrogenation reactions were observed for the B-methylated analogues. This is suggested to be a consequence of the increased hydridic nature of the hydrogen atoms at boron induced by the electron donating methyl group.

Attempts to synthesize high molecular weight polyaminoboranes with a methyl substituent at boron were made via catalytic dehydropolymerization of **1a** and **1b**. However, any oligomeric or polymeric B-methylated species that formed under the reaction conditions appeared to readily undergo further dehydrogenation to yield mainly the B-methylated borazine, $[\text{RN}=\text{BMe}]_3$ ($\text{R} = \text{H}, \text{Me}$). We are continuing our efforts in this area with the aim to increase the yield of poly(B-methyl aminoborane) and other analogous materials under conditions where further dehydrocoupling is absent.

Very rapid hydrogenation of $i\text{Pr}_2\text{N}=\text{BH}_2$ to $i\text{Pr}_2\text{NH}\cdot\text{BH}_3$ was observed for the B-methylated amine-borane, **1a**, with complete hydrogen transfer observed after 10 min in THF at 20 °C, with very good hydrogenation rates also observed for **1b** and **1c**. The hydrogen donating ability of B-methylated amine-

boranes was significantly increased compared to amine-boranes without a methyl group at boron. DFT calculations revealed that the pathway for hydrogen transfer occurred via a cyclic six-membered transition state. In addition, the reaction was determined to be exergonic with a lower activation energy barrier than for our previous model using $\text{Me}_2\text{NH}\cdot\text{BH}_3$ as the hydrogen donor. These results show that, both kinetically and thermodynamically, B-methylated amine-boranes **1a–1c** have an improved hydrogen donating ability toward the amino-borane $i\text{Pr}_2\text{N}=\text{BH}_2$ than the previously investigated amine-borane, $\text{Me}_2\text{NH}\cdot\text{BH}_3$. Our ongoing studies focus on transfer hydrogenations involving B-methylated amine-boranes with unsaturated organic substrates.

■ ASSOCIATED CONTENT

Supporting Information

The Supporting Information is available free of charge on the ACS Publications website at DOI: 10.1021/acs.inorgchem.5b01946.

Details of all experiments along with NMR spectra, mass spectra, elemental analysis, crystallographic information and DFT studies (PDF)

Crystallographic information for **1a**, CH_8BN (CIF)

Crystallographic information for **1b**, $\text{C}_2\text{H}_{10}\text{BN}$ (CIF)

Crystallographic information for **1d**, $\text{C}_7\text{H}_{20}\text{BN}$ (CIF)

■ AUTHOR INFORMATION

Corresponding Author

*E-mail: Ian.Manners@bristol.ac.uk.

Notes

The authors declare no competing financial interest.

■ ACKNOWLEDGMENTS

N.E.S., A.S., A.P.M.R., and I.M. acknowledge EPSRC for funding. A.S. is grateful to the Deutsche Forschungsgemeinschaft (DFG) for a postdoctoral research fellowship. E.M.L. and T.J. acknowledge the EU for Marie Curie Postdoctoral Fellowships.

■ REFERENCES

- (a) Leitao, E. M.; Jurca, T.; Manners, I. *Nat. Chem.* **2013**, *5*, 817–829. (b) Staubitz, A.; Robertson, A. P. M.; Sloan, M. E.; Manners, I. *Chem. Rev.* **2010**, *110*, 4023–4078. (c) Staubitz, A.; Robertson, A. P. M.; Manners, I. *Chem. Rev.* **2010**, *110*, 4079–4124. (d) Smythe, N. C.; Gordon, J. C. *Eur. J. Inorg. Chem.* **2010**, *2010*, 509–521. (e) Sutton, A. D.; Burrell, A. K.; Dixon, D. A.; Garner, E. B.; Gordon, J. C.; Nakagawa, T.; Ott, K. C.; Robinson, P.; Vasiliu, M. *Science* **2011**, *331*, 1426–1429. (f) Liu, Z.; Marder, T. B. *Angew. Chem., Int. Ed.* **2008**, *47*, 242–244. (g) Stephens, F. H.; Pons, V.; Baker, R. T. *Dalton Trans.* **2007**, 2613–2626. (h) Johnson, H. C.; Hooper, T. N.; Weller, A. S. *Top. Organomet. Chem.* **2015**, *49*, 153–220. (i) Robertson, A. P. M.; Leitao, E. M.; Manners, I. *J. Am. Chem. Soc.* **2011**, *133*, 19322–19325. (j) Leitao, E. M.; Stubbs, N. E.; Robertson, A. P. M.; Helten, H.; Cox, R. J.; Lloyd-Jones, G. C.; Manners, I. *J. Am. Chem. Soc.* **2012**, *134*, 16805–16816. (k) Yang, X.; Zhao, L.; Fox, T.; Wang, Z.-X.; Berke, H. *Angew. Chem., Int. Ed.* **2010**, *49*, 2058–2062. (l) Yang, X.; Fox, T.; Berke, H. *Org. Biomol. Chem.* **2012**, *10*, 852–860. (m) Jaska, C. A.; Manners, I. *J. Am. Chem. Soc.* **2004**, *126*, 2698–2699. (n) Sloan, M. E.; Staubitz, A.; Lee, K.; Manners, I. *Eur. J. Org. Chem.* **2011**, *2011*, 672–675. (o) Chen, X.; Zhao, J.-C.; Shore, S. G. *J. Am. Chem. Soc.* **2010**, *132*, 10658–10659.
- (a) Liu, Z.; Song, L.; Zhao, S.; Huang, J.; Ma, L.; Zhang, J.; Lou, J.; Ajayan, P. M. *Nano Lett.* **2011**, *11*, 2032–2037. (b) Kim, D.-P.; Moon, K.-T.; Kho, J.-G.; Economy, J.; Gervais, C.; Babonneau, F. *Polym. Adv. Technol.* **1999**, *10*, 702–712. (c) Nakhmanson, S. M.; Nardelli, M. B.; Bernholc, J. *Phys. Rev. Lett.* **2004**, *92*, 115504. (d) Staubitz, A.; Presa Soto, A.; Manners, I. *Angew. Chem., Int. Ed.* **2008**, *47*, 6212–6215.
- (a) Whittell, G. R.; Balmond, E. I.; Robertson, A. P. M.; Patra, S. K.; Haddow, M. F.; Manners, I. *Eur. J. Inorg. Chem.* **2010**, *2010*, 3967–3975. (b) Miller, A. J. M.; Bercaw, J. E. *Chem. Commun.* **2010**, *46*, 1709–1711. (c) Appelt, C.; Slootweg, J. C.; Lammertsma, K.; Uhl, W. *Angew. Chem., Int. Ed.* **2013**, *52*, 4256–4259.
- (a) Jaska, C. A.; Temple, K.; Lough, A. J.; Manners, I. *J. Am. Chem. Soc.* **2003**, *125*, 9424–9434. (b) Douglas, T. M.; Chaplin, A. B.; Weller, A. S. *J. Am. Chem. Soc.* **2008**, *130*, 14432–14433. (c) Tang, C. Y.; Thompson, A. L.; Aldridge, S. J. *J. Am. Chem. Soc.* **2010**, *132*, 10578–10591. (d) Tang, C. Y.; Thompson, A. L.; Aldridge, S. *Angew. Chem., Int. Ed.* **2010**, *49*, 921–925. (e) Dallanegra, R.; Robertson, A. P. M.; Chaplin, A. B.; Manners, I.; Weller, A. S. *Chem. Commun.* **2011**, *47*, 3763–3765. (f) Johnson, H. C.; Leitao, E. M.; Whittell, G. R.; Manners, I.; Lloyd-Jones, G. C.; Weller, A. S. *J. Am. Chem. Soc.* **2014**, *136*, 9078–9093. (g) Sewell, L. J.; Lloyd-Jones, G. C.; Weller, A. S. *J. Am. Chem. Soc.* **2012**, *134*, 3598–3610. (h) Zahmakiran, M.; Özkaz, S. *Inorg. Chem.* **2009**, *48*, 8955–8964. (i) Chen, Y.; Fulton, J. L.; Linehan, J. C.; Autrey, T. *J. Am. Chem. Soc.* **2005**, *127*, 3254–3255.
- (a) Denney, M. C.; Pons, V.; Hebden, T. J.; Heinekey, D. M.; Goldberg, K. I. *J. Am. Chem. Soc.* **2006**, *128*, 12048–12049. (b) Dietrich, B. L.; Goldberg, K. I.; Heinekey, D. M.; Autrey, T.; Linehan, J. C. *Inorg. Chem.* **2008**, *47*, 8583–8585. (c) Staubitz, A.; Sloan, M. E.; Robertson, A. P. M.; Friedrich, A.; Schneider, S.; Gates, P. J.; Schmedt auf der Günne, J. S.; Manners, I. *J. Am. Chem. Soc.* **2010**, *132*, 13332–13345. (d) Stevens, C. J.; Dallanegra, R.; Chaplin, A. B.; Weller, A. S.; Macgregor, S. A.; Ward, B.; McKay, D.; Alcaraz, G.; Sabo-Etienne, S. *Chem. - Eur. J.* **2011**, *17*, 3011–3020.
- (a) Robertson, A. P. M.; Suter, R.; Chabanne, L.; Whittell, G. R.; Manners, I. *Inorg. Chem.* **2011**, *50*, 12680–12691. (b) Vogt, M.; de Bruin, B.; Berke, H.; Trincado, M.; Grützmacher, H. *Chem. Sci.* **2011**, *2*, 723–727. (c) Keaton, R. J.; Blacquire, J. M.; Baker, R. T. *J. Am. Chem. Soc.* **2007**, *129*, 1844–1845.
- (a) Sloan, M. E.; Staubitz, A.; Clark, T. J.; Russell, C. A.; Lloyd-Jones, G. C.; Manners, I. *J. Am. Chem. Soc.* **2010**, *132*, 3831–3841. (b) Helten, H.; Dutta, B.; Vance, J. R.; Sloan, M. E.; Haddow, M. F.; Sproules, S.; Collison, D.; Whittell, G. R.; Lloyd-Jones, G. C.; Manners, I. *Angew. Chem., Int. Ed.* **2013**, *52*, 437–440.
- (a) Vance, J. R.; Robertson, A. P. M.; Lee, K.; Manners, I. *Chem. - Eur. J.* **2011**, *17*, 4099–4103. (b) Vance, J. R.; Schäfer, A.; Robertson, A. P. M.; Lee, K.; Turner, J.; Whittell, G. R.; Manners, I. *J. Am. Chem. Soc.* **2014**, *136*, 3048–3064. (c) Baker, R. T.; Gordon, J. C.; Hamilton, C. W.; Henson, N. J.; Lin, P.-H.; Maguire, S.; Murugesu, M.; Scott, B. L.; Smythe, N. C. *J. Am. Chem. Soc.* **2012**, *134*, 5598–5609. (d) Bhattacharya, P.; Krause, J. P.; Guan, H. *J. Am. Chem. Soc.* **2014**, *136*, 11153–11161. (e) Luo, W.; Campbell, P. G.; Zakharov, L. N.; Liu, S.-Y. *J. Am. Chem. Soc.* **2011**, *133*, 19326–19329. (f) Luo, W.; Campbell, P. G.; Zakharov, L. N.; Liu, S.-Y. *J. Am. Chem. Soc.* **2013**, *135*, 8760–8760. (g) Lichtenberg, C.; Viciu, L.; Adelhardt, M.; Sutter, J.; Meyer, K.; de Bruin, B.; Grützmacher, H. *Angew. Chem., Int. Ed.* **2015**, *54*, 5766–5771.
- (a) Jiang, Y.; Berke, H. *Chem. Commun.* **2007**, 3571–3573. (b) Jiang, Y. F.; Blacque, O.; Fox, T.; Frech, C. M.; Berke, H. *Organometallics* **2009**, *28*, 5493–5504.
- (a) Friedrich, A.; Drees, M.; Schneider, S. *Chem. - Eur. J.* **2009**, *15*, 10339–10342. (b) Käß, M.; Friedrich, A.; Drees, M.; Schneider, S. *Angew. Chem., Int. Ed.* **2009**, *48*, 905–907. (c) Marziale, A. N.; Friedrich, A.; Klopsch, I.; Drees, M.; Celinski, V. R.; Schmedt auf der Günne, J. S.; Schneider, S. *J. Am. Chem. Soc.* **2013**, *135*, 13342–13355.
- (a) Waterman, R. *Chem. Soc. Rev.* **2013**, *42*, 5629–5641. (b) Hill, M. S.; Kociok-Köhne, G.; Robinson, T. P. *Chem. Commun.* **2010**, *46*, 7587–7589. (c) Buss, J. A.; Edouard, G. A.; Cheng, C.; Shi, J.; Agapie, T. *J. Am. Chem. Soc.* **2014**, *136*, 11272–11275. (d) Campbell, P. G.; Ishibashi, J. S. A.; Zakharov, L. N.; Liu, S.-Y. *Aust. J. Chem.* **2014**, *67*, 521–524. (e) Mal, S. S.; Stephens, F. H.; Baker, R. T. *Chem. Commun.* **2011**, *47*, 2922–2924. (f) Chen, G.;

- Zakharov, L. N.; Bowden, M. E.; Karkamkar, A. J.; Whittemore, S. M.; Garner, E. B., III; Mikulas, T. C.; Dixon, D. A.; Autrey, T.; Liu, S.-Y. *J. Am. Chem. Soc.* **2015**, *137*, 134–137.
- (12) (a) Ewing, W. C.; Marchione, A.; Himmelberger, D. W.; Carroll, P. J.; Sneddon, L. G. *J. Am. Chem. Soc.* **2011**, *133*, 17093–17099. (b) Harder, S.; Spielmann, J. *Chem. Commun.* **2011**, 47, 11945–11947. (c) Bellham, P.; Hill, M. S.; Kociok-Köhn, G. *Organometallics* **2014**, *33*, 5716–5721. (d) Erickson, K. A.; Wright, D. S.; Waterman, R. J. *Organomet. Chem.* **2014**, *751*, 541–545. (e) Stephens, F. H.; Baker, R. T.; Matus, M. H.; Grant, D. J.; Dixon, D. A. *Angew. Chem., Int. Ed.* **2007**, *46*, 746–749. (f) Hansmann, M. M.; Melen, R. L.; Wright, D. S. *Chem. Sci.* **2011**, *2*, 1554–1559.
- (13) Bhunya, S.; Malakar, T.; Paul, A. *Chem. Commun.* **2014**, *50*, 5919–5922.
- (14) (a) Johnson, H. C.; Robertson, A. P. M.; Chaplin, A. B.; Sewell, L. J.; Thompson, A. L.; Haddow, M. F.; Manners, I.; Weller, A. S. *J. Am. Chem. Soc.* **2011**, *133*, 11076–11079. (b) Johnson, H. C.; Robertson, A. P. M.; Chaplin, A. B.; Sewell, L. J.; Thompson, A. L.; Haddow, M. F.; Manners, I.; Weller, A. S. *J. Am. Chem. Soc.* **2012**, *134*, 3932–3932.
- (15) Bhunya, S.; Zimmerman, P. M.; Paul, A. *ACS Catal.* **2015**, *5*, 3478–3493.
- (16) Wu, D.; Li, Y.; Ganguly, R.; Kinjo, R. *Chem. Commun.* **2014**, *50*, 12378–12381.
- (17) (a) Chong, C. C.; Hirao, H.; Kinjo, R. *Angew. Chem., Int. Ed.* **2014**, *53*, 3342–3346. (b) Dunn, N. L.; Ha, M. J.; Radosevich, A. T. *J. Am. Chem. Soc.* **2012**, *134*, 11330–11333.
- (18) Anane, H.; Jarid, A.; Boutalib, A.; Nebot-Gil, I.; Tomás, F. J. *Mol. Struct.: THEOCHEM* **1998**, *455*, 51–57.
- (19) Grant, D. J.; Matus, M. H.; Anderson, K. D.; Camaioni, D. M.; Neufeldt, S. R.; Lane, C. F.; Dixon, D. A. *J. Phys. Chem. A* **2009**, *113*, 6121–6132.
- (20) Robertson, A. P. M.; Whittell, G. R.; Staubitz, A.; Lee, K.; Lough, A. J.; Manners, I. *Eur. J. Inorg. Chem.* **2011**, *2011*, 5279–5287.
- (21) Robertson, A. P. M.; Haddow, M. F.; Manners, I. *Inorg. Chem.* **2012**, *51*, 8254–8264.
- (22) Paul, V.; Roberts, B. P. *J. Chem. Soc., Perkin Trans. 2* **1988**, 1183–1193.
- (23) Beachley, O. T.; Washburn, B. *Inorg. Chem.* **1975**, *14*, 120–123.
- (24) Singaram, B.; Cole, T. E.; Brown, H. C. *Organometallics* **1984**, *3*, 774–777.
- (25) See the [Supporting Information](#) for further details.
- (26) Ortmann, R.; Schlitzer, M. *Synthesis* **2009**, *2009*, 1757–1759.
- (27) Klooster, W. T.; Koetzle, T. F.; Siegbahn, P. E. M.; Richardson, T. B.; Crabtree, R. H. *J. Am. Chem. Soc.* **1999**, *121*, 6337–6343.
- (28) Aldridge, S.; Downs, A. J.; Tang, C. Y.; Parsons, S.; Clarke, M. C.; Johnstone, R. D. L.; Robertson, H. E.; Rankin, D. W. H.; Wann, D. A. *J. Am. Chem. Soc.* **2009**, *131*, 2231–2243.
- (29) (a) Helten, H.; Robertson, A. P. M.; Staubitz, A.; Vance, J. R.; Haddow, M. F.; Manners, I. *Chem. - Eur. J.* **2012**, *18*, 4665–4680. (b) Crabtree, R. H.; Siegbahn, P. E. M.; Eisenstein, O.; Rheingold, A. L.; Koetzle, T. F. *Acc. Chem. Res.* **1996**, *29*, 348–354.
- (30) Wrackmeyer, B.; Tok, O. L. Z. *Naturforsch., B: J. Chem. Sci.* **2007**, *62*, 220–224.
- (31) Nöth, H.; Rojas-Lima, S.; Troll, A. *Eur. J. Inorg. Chem.* **2005**, *2005*, 1895–1906.
- (32) Narula, C. K.; Janik, J. F.; Duesler, E. N.; Paine, R. T.; Schaeffer, R. *Inorg. Chem.* **1986**, *25*, 3346–3349.
- (33) Jaska, C. A.; Manners, I. *J. Am. Chem. Soc.* **2004**, *126*, 9776–9785.
- (34) (a) Borazine [MeN–BMe]₃ was independently synthesized through dehydrocoupling MeNH₂·BH₂Me with 100 mol % Ni, and characterized by ¹¹B, ¹H, and ¹³C NMR spectroscopies and EI-MS ([Figures S12–S15](#)). (b) Smalley, J. H.; Stafiej, S. F. *J. Am. Chem. Soc.* **1959**, *81*, 582–586. (c) Haworth, D. T.; Hohnstedt, L. F. *J. Am. Chem. Soc.* **1960**, *82*, 3860–3862.
- (35) Assignment of [RNH–BHMe]_x (R = H, Me) was made by comparing the difference in ¹¹B chemical shifts of NH₃·BH₂Me [$\delta_{B,exp}$ –15.1] and NH₃·BH₃ [$\delta_{B,lit}$ –21.6]^{4a} to [RNH–BH₂]_n [R = H, $\delta_{B,lit}$ –21.0 and –10.7] [R = Me, $\delta_{B,lit}$ –6.5]^{5c}.
- (36) Stubbs, N. E.; Jurca, T.; Leitao, E. M.; Woodall, C. H.; Manners, I. *Chem. Commun.* **2013**, 49, 9098–9100.
- (37) (a) Pons, V.; Baker, R. T.; Szymczak, N. K.; Heldebrant, D. J.; Linehan, J. C.; Matus, M. H.; Grant, D. J.; Dixon, D. A. *Chem. Commun.* **2008**, 6597–6599. (b) Chapman, A. M.; Haddow, M. F.; Wass, D. F. *J. Am. Chem. Soc.* **2011**, *133*, 8826–8829. (c) Malakar, T.; Bhunya, S.; Paul, A. *Chem. - Eur. J.* **2015**, *21*, 6340–6345.
- (38) Cotton, F. A.; Wilkinson, G.; Gaus, P. L. *Basic Inorganic Chemistry*, 3rd ed.; John Wiley & Sons, Inc.: New York, 1995; pp 326–327.
- (39) Pasto, D. J.; Lepeska, B.; Balasubramanian, V. *J. Am. Chem. Soc.* **1972**, *94*, 6090–6096.
- (40) (a) Hartman, J. S.; Miller, J. M. *Inorg. Nucl. Chem. Lett.* **1969**, *5*, 831–835. (b) Benton-Jones, B.; Davidson, M. E. A.; Hartman, J. S.; Klassen, J. J.; Miller, J. M. *J. Chem. Soc., Dalton Trans.* **1972**, 2603–2607. (c) Krishnamurthy, S. S.; Lappert, M. F. *Inorg. Nucl. Chem. Lett.* **1971**, *7*, 919–925. (d) Hofmeister, H. K.; Van Wazer, J. R. *J. Inorg. Nucl. Chem.* **1964**, *26*, 1209–1213.
- (41) Benton, B. W.; Miller, J. M. *Can. J. Chem.* **1974**, *52*, 2866–2872.
- (42) (a) Miertuš, S.; Scrocco, E.; Tomasi, J. *Chem. Phys.* **1981**, *55*, 117–129. (b) Miertuš, S.; Tomasi, J. *Chem. Phys.* **1982**, *65*, 239–245. (c) Pascual-Ahuir, J. L.; Silla, E.; Tuñón, I. *J. Comput. Chem.* **1994**, *15*, 1127–1138. (d) Tomasi, J.; Mennucci, B.; Cammi, R. *Chem. Rev.* **2005**, *105*, 2999–3094.
- (43) Shahriari-Zavareh, H.; Stoddart, J. F.; Williams, M. K.; Allwood, B. L.; Williams, D. J. *J. Inclusion Phenom.* **1985**, *3*, 355–377.
- (44) Jaska, C. A.; Clark, T. J.; Clendenning, S. B.; Grozea, D.; Turak, A.; Lu, Z.-H.; Manners, I. *J. Am. Chem. Soc.* **2005**, *127*, S116–S124.
- (45) Reactions were performed under conditions analogous to those previously reported,^{11j} with the percentage of hydrogenation calculated via integration of *i*Pr₂N=BH₂ and *i*Pr₂NH·BH₃ by ¹¹B NMR spectroscopy.
- (46) Previous DFT calculations investigating the hydrogen transfer mechanism between Me₂NH·BH₃ and *i*Pr₂N=BH₂ were performed at the PBE0/6-31G(d,p) level of theory.^{1j}
- (47) We considered another possible route to *i*Pr₂N=BHMe which involves the formation of **1d** by redistribution, followed by dehydrogenation. However, by ¹¹B NMR spectroscopy any redistribution reaction between *i*Pr₂NH·BH₃ and **1a** to form **1d** in THF was negligible on the time scale of the reaction: see [Figure S60](#).